

PLENTY, a hydroxyproline
O-arabinosyltransferase, negatively regulates
root nodule symbiosis in *Lotus japonicus*

著者 (英)	Emiko Yoro, Hanna Nishida, Mari Ogawa-Ohnishi, Chie Yoshida, Takuya SUZAKI, Yoshikatsu Matsubayashi, Masayoshi Kawaguchi
journal or publication title	Journal of Experimental Botany
volume	70
number	2
page range	507-517
year	2019-01
権利	(C) The Author(s) 2018. Published by Oxford University Press on behalf of the Society for Experimental Biology This is an Open Access article distributed under the terms of the Creative Commons Attribution License (http://creativecommons.org/licenses/by/4.0/), which permits unrestricted reuse, distribution, and reproduction in any medium, provided the original work is properly cited.
URL	http://hdl.handle.net/2241/00155414

doi: 10.1093/jxb/ery364



RESEARCH PAPER

PLENTY, a hydroxyproline O-arabinoxyltransferase, negatively regulates root nodule symbiosis in *Lotus japonicus*

Emiko Yoro^{1,2,*}, Hanna Nishida^{1,3}, Mari Ogawa-Ohnishi⁴, Chie Yoshida¹, Takuya Suzuki^{1,2,3}, Yoshikatsu Matsubayashi⁴ and Masayoshi Kawaguchi^{1,2,†}

¹ Division of Symbiotic Systems, National Institute for Basic Biology, Okazaki, Aichi 444-8585, Japan

² Department of Basic Biology, School of Life Science, Graduate University for Advanced Studies (SOKENDAI), Okazaki, Aichi 444-8585, Japan

³ Graduate School of Life and Environmental Sciences, University of Tsukuba, Tsukuba, Ibaraki 305-8577, Japan

⁴ Division of Biological Science, Graduate School of Science, Nagoya University Chikusa, Nagoya 464-8601, Japan

* Present address: Department of Life Science, Rikkyo University, Tokyo, 171-8501, Japan.

† Correspondence: masayosi@nibb.ac.jp

Received 21 March 2018; Editorial decision 12 October 2018; Accepted 18 October 2018

Editor: Miriam Gifford, University of Warwick, UK

Abstract

Legumes can survive in nitrogen-deficient environments by forming root-nodule symbioses with rhizobial bacteria; however, forming nodules consumes energy, and nodule numbers must thus be strictly controlled. Previous studies identified major negative regulators of nodulation in *Lotus japonicus*, including the small peptides CLAVATA3/ESR (CLE)-RELATED-ROOT SIGNAL1 (CLE-RS1), CLE-RS2, and CLE-RS3, and their putative major receptor HYPERNODULATION AND ABERRANT ROOT FORMATION1 (HAR1). CLE-RS2 is known to be expressed in rhizobia-inoculated roots, and is predicted to be post-translationally arabinosylated, a modification essential for its activity. Moreover, all three CLE-RSs suppress nodulation in a HAR1-dependent manner. Here, we identified PLENTY as a gene responsible for the previously isolated hypernodulation mutant *plenty*. PLENTY encoded a hydroxyproline O-arabinoxyltransferase orthologous to ROOT DETERMINED NODULATION1 in *Medicago truncatula*. PLENTY was localized to the Golgi, and an *in vitro* analysis of the recombinant protein demonstrated its arabinosylation activity, indicating that CLE-RS1/2/3 may be substrates for PLENTY. The constitutive expression experiments showed that CLE-RS3 was the major candidate substrate for PLENTY, suggesting the substrate preference of PLENTY for individual CLE-RS peptides. Furthermore, a genetic analysis of the *plenty har1* double mutant indicated the existence of another PLENTY-dependent and HAR1-independent pathway negatively regulating nodulation.

Keywords: Arabinosyltransferase, CLE peptide, glycosylation, legume–rhizobial symbiosis, *Lotus japonicus*, nodulation control, post-translational modification.

Introduction

Legumes have evolved the ability to make specialized root organs called nodules, in which nitrogen-fixing symbionts, rhizobial bacteria, reside. This symbiosis enables legumes to grow on nitrogen-limited soils; however, the beneficial nitrogen acquisition is balanced against the high energy inputs required to fuel cell division in the nodules, as well as the allocation

of photoassimilates to the rhizobia (Udvardi and Poole, 2013). Legumes have therefore developed mechanisms for maintaining the symbiotic balance between forming nodules to satisfy their nitrogen requirements and sustaining the energy levels required for other biological processes; these mechanisms are termed the autoregulation of nodulation (AON) (Kosslak and Bohlool, 1984; Caetano-Anollés and Gresshoff, 1990, 1991). The potential AON mechanisms involving systemic signaling between the root and shoot were originally determined using split-root and grafting techniques (Kosslak and Bohlool, 1984; Delves *et al.*, 1986), and the molecules participating in the negative control of nodulation have been elucidated (reviewed by (Magori and Kawaguchi, 2009; Reid *et al.*, 2011b; Suzuki *et al.*, 2015).

The current plausible model of AON via a systemic root-derived signal involves the expression of the systemic negative regulators, such as *CLAVATA3/ESR* (*CLE-RELATED-ROOT SIGNAL1* (*CLE-RS1*), *CLE-RS2*, and *CLE-RS3* in *Lotus japonicus*, directly induced by transcription factors, NODULE INCEPTION (NIN) or NIN-like protein NITRATE UNRESPONSIVE SYMBIOSIS1 (NRSYM1) (Soyano *et al.*, 2014; Nishida *et al.*, 2016; Nishida and Suzuki, 2018; Nishida *et al.*, 2018). Other related *CLE* peptides negatively regulating nodulation have also been found in *L. japonicus* and other legumes, including *Medicago truncatula*, pea (*Pisum sativum*), and soybean (*Glycine max*) (Mortier *et al.*, 2010). Other AON factors closely related to PLENTY, namely ROOT DETERMINED NODULATION1 (RDN1) and NODULATION3 (NOD3), were found in *M. truncatula* and in pea, respectively. MtRDN1 and PsNOD3 are orthologous and have been suggested as factors that function in the root but not in the shoot (Li *et al.*, 2009; Novák, 2010; Schnabel *et al.*, 2011; Osipova *et al.*, 2012; Kassaw *et al.*, 2017), but their molecular functions had been unclear. Prior to the functional identification of *MtRDN1/PsNOD3*, their Arabidopsis homologs were reported as hydroxyproline O-arabinosyltransferases (HPATs) and termed HPAT1 (At2g25260), HPAT2 (At5g13500), and HPAT3 (At5g25265), which have recently been classified into the GT95 glycosyltransferase family (Showalter and Basu, 2016). *At*HPATs redundantly contribute to transferring an L-arabinosyl residue to the hydroxyl group of the hydroxyproline residues of several substrates, including extensin, *At*CLE2, and Arabidopsis plant peptide containing sulfated tyrosine 1 (*At*PSY1) (Ogawa-Ohnishi *et al.*, 2013; MacAlister *et al.*, 2016). This discovery raised the possibility that *Lj*PLENTY, *MtRDN1*, or *PsNOD3* mediates the arabinosylation of their *CLE* peptides functioning in AON in the respective species. Additionally, a recent study of the *MtRDN*s reported that, of the two *CLE* peptides, only *MtCLE12* is required for a functional *MtRDN1* to repress nodulation, suggesting that *MtRDN1* post-translationally modifies *MtCLE12* but not *MtCLE13* (Kassaw *et al.*, 2017).

The *plenty* mutant was previously isolated as a hypernodulator, but the gene responsible for this phenotype has not yet been identified (Yoshida *et al.*, 2010). Here, we identify the *plenty* locus and characterize PLENTY as an ortholog of *MtRDN1* and *PsNOD3* (Postma *et al.*, 1988; Sagan and Duc, 1996; Schnabel *et al.*, 2011). We determine the localization of PLENTY to the Golgi and purified recombinant PLENTY protein to detect its HPAT activity. This biochemical assay using an artificially synthesized

peptide as a substrate for arabinosylation provided direct molecular evidence that PLENTY acts as a post-translational modification HPAT enzyme. Furthermore, the constitutive expression of *CLE-RS1/2/3* in *plenty* suggested that PLENTY preferentially associates with *CLE-RS3* peptides as substrate. Finally, *plenty har1* double mutant analysis indicates the existence of an unknown substrate for PLENTY other than *CLE-RS1/2/3*, which is not accepted by HAR1. These findings provide a molecular clue for understanding how PLENTY regulates nodulation.

Materials and methods

Growth conditions

Lotus japonicus (Miyakojima MG-20) seeds were sown in sterilized vermiculite, to which Broughton and Dilworth (B&D) solution (Broughton and Dilworth, 1971) containing 0.5 mM KNO₃. Seeds were inoculated with *Mesorhizobium loti* MAFF303099, while the control seedlings were not inoculated. Seedlings were grown under 16 h light/8 h dark cycles at 24 °C.

Map-based cloning, genomic PCR, and 5'-/3'-RACE

The *plenty* mutants were backcrossed three times to the parental plant 'Miyakojima MG-20' and crossed with another accession, 'Gifu B-129'. DNA polymorphisms in the genomes of the 1087 F₂ progeny displaying the *plenty* mutant phenotype were identified using a series of genetic markers (http://www.kazusa.or.jp/lotus/markerdb_index.html, last accessed 25 October 2018) and two genetic markers newly developed in this study, EY004 and EY005 (see Supplementary Table S1 at JXB online). Genomic DNA was extracted with a DNeasy Plant Mini Kit (Qiagen). The ~16 kb deletion in the *plenty* mutant was identified using genomic PCR (Supplementary Fig. S1), with the sets of primers shown in Supplementary Table S2. The 5' and 3' ends of PLENTY, PLENTY2, and PLENTY3 were determined using a SMARTer[®] RACE cDNA Amplification Kit (Clontech), utilizing RNA extracted from whole roots inoculated with *M. loti* MAFF303099. The DDBJ accession numbers for the PLENTY, PLENTY2, and PLENTY3 mRNAs were LC010646–LC010648 (<http://getentry.ddbj.nig.ac.jp/top-e.html>, last accessed 25 October 2018).

Plasmid construction

A deletion series of PLENTY coding sequence (CDS), as well as a full-length CDS, were generated using reverse transcription and the appropriate primer sets (Supplementary Table S2), cloned into the pGEM[®]-T-Easy vector (Promega) using the TA strategy, and named pGEM-Full-PLENTY, pGEM-ΔN1-PLENTY, and pGEM-N-PLENTY. The full-length CDS clone starts at the seventh predicted codon of PLENTY compared with the previous report of *MtRDN1* (Schnabel *et al.*, 2011; Supplementary Appendix S2); at the time it was generated, that was the predicted start of the CDS. Next, each construct was digested with *Eco*RI and *Spe*I, inserted into the Gateway-based entry plasmid pJL-Blue (Suzuki *et al.*, 2012), and named pJL-Blue-Full-PLENTY, pJL-Blue-ΔN1-PLENTY, and pJL-Blue-N-PLENTY, respectively. For the complementation test, full-length PLENTY CDS fragments were inserted into the Gateway site of pUB-GW-HYG using an LR recombination reaction (Invitrogen) to generate pUB-GW-Full-PLENTY (Maekawa *et al.*, 2008). To produce PLENTY-green fluorescent protein (GFP) fusion proteins, the stop codon of each pJL-Blue-based entry vector was mutagenized using circular PCR with a phosphorylated set of primers (Supplementary Table S2), and the vector was then digested with *Dpn*I and self-ligated. The subcellular localization of PLENTY was analyzed using a series of PLENTY fragments from the mutagenized pJL-Blue-based entry vectors, which were inserted into pUGW5 for particle bombardment into onion (*Allium cepa*) epidermal cells and *L. japonicus* roots. The PLENTY fragments were also inserted into pGW5 for the *Agrobacterium tumefaciens*-mediated infiltration of *Nicotiana benthamiana* using an LR recombination reaction (Invitrogen).

The two constructs, pUGW5 and pGWB5 (Nakagawa *et al.*, 2007), were kindly provided by Dr Mano (National Institute for Basic Biology) and Dr Nakagawa (Shimane University), respectively. To detect the HPAT activities of the three *PLENTY* CDS fragments (full-length, Δ N1, and Δ N2), they were C-terminally fused to a FLAG tag using pGEM-Full-*PLENTY* as a template for the PCR (see [Supplementary Table S2](#) for the list of primers). The fragments were inserted into pYES2 (Invitrogen) and linearized with *Bam*HI in an In-Fusion reaction (Takara). The plasmids used for the constitutive expression of *GUS* (β -glucuronidase), *CLE3*, *CLE-RS1/2* (Okamoto *et al.*, 2009) and *CLE-RS3* (Nishida *et al.*, 2016) were previously described.

Hairy root and stable transformations of *L. japonicus*

Hairy root and stable transformations of *L. japonicus* were performed using the *Agrobacterium rhizogenes* strain AR1193 alone or in combination with the *Agrobacterium tumefaciens* strain AGL1 harboring the respective plasmids, as described previously (<http://www.bio-protocol.org/wenzhang.aspx?id=795>, <http://www.bio-protocol.org/wenzhang.aspx?id=796>, last accessed 25 October 2018). In the hairy root transformations constitutively expressing *GUS*, *CLE3*, and *CLE-RS1/2/3*, GFP fluorescence was used as a marker of transformation, and the successfully transformed roots were inoculated with *M. loti* MAFF303099. The nodule numbers and other phenotypes of the hairy roots and stably transformed roots were measured at 14 days after inoculation (DAI), while the growth phenotypes of the stable transformants were measured at 8 weeks after inoculation.

Phylogenetic analysis

Forty-one amino acid sequences were obtained from the study of *MtRDN1* (Schnabel *et al.*, 2011) and an additional 16 amino acid sequences of *Brassica rapa* Chiifu-401 v1.2, *Carica papaya* ASGPB v0.4, *Gossypium raimondii* v2.1, and *Eucalyptus grandis* v2.0 genomes were obtained from a BLAST search for the Phytozome website (<http://www.phytozome.net/>, last accessed 25 October 2018). The total 57 amino acid sequences were aligned using MUSCLE (Edgar, 2004). All positions containing gaps and missing data were eliminated, and the final data set comprised a total of 266 amino acid positions. Evolutionary analyses were conducted in MEGA6 (Tamura *et al.*, 2013). The evolutionary history was inferred using the Maximum Likelihood method, based on the Le_Gascuel_2008 model (Le and Gascuel, 2008). The tree with the highest log likelihood (-7013.2051) is shown in [Supplementary Fig. S2](#). The initial tree for the heuristic search was obtained by applying the Neighbor-Joining method to a matrix of pairwise distances estimated using the JTT model. A discrete Gamma distribution was used to model the evolutionary rate differences between the sites [five categories (+G, parameter=0.4454)].

Subcellular localization analysis

Onion epidermal cells and *L. japonicus* roots of 3-day-old seedlings grown on moistened filter paper were transformed with each construct (pUGW5-based series) via particle bombardment with a Helios Gene Gun (BIO-RAD), as described previously (Mano *et al.*, 2006). To verify the co-localization of proteins with the Golgi network, *A. tumefaciens* AGL1 strains carrying each construct (pGWB5-based series) and an mCherry-fused Golgi marker construct (G-rb) (Nelson *et al.*, 2007) were mixed and co-infiltrated into *Nicotiana benthamiana* leaves using a p19-harboring strain, as previously described (Voinnet *et al.*, 2003; Kinoshita *et al.*, 2010).

Microscopy observations

Bright-field and fluorescence images were generated using an SZX12/16 stereomicroscope or a BX50 microscope (Olympus) and a DP Controller (Olympus). Confocal images were generated using an A1 confocal laser-scanning microscope (Nikon) with a $\times 10$ or $\times 20/0.75$ NA objective lens.

Detection of HPAT activity in *PLENTY*

PLENTY proteins were expressed as a C-terminal FLAG-tag fusion in the yeast (*Saccharomyces cerevisiae*) strain INVSc1, which was transformed with pYES2 vectors (Invitrogen) harboring full-length *PLENTY* or one of the two N-terminally deleted *PLENTY* constructs. Their expression was detected using immunoblotting, and the proteins were collected within a pellet of microsomal membrane, as described previously (Ogawa-Ohnishi *et al.*, 2013). HPAT activity assays were performed in 20 μ l reaction mixtures containing 100 mM MOPS-KOH (pH 7.0) buffer, 1 mM $MnCl_2$, 1.0% Triton X-100, 250 μ M UDP- β -L-arabinofuranose (Peptide Institute, Inc.), 100 μ M (PGVOOS)₃ peptide, and 150 μ g of total yeast microsomal membrane. The reaction mixture was incubated at 30 °C for 2 h, and then terminated by the addition of 100 μ l of 0.1% formic acid. After centrifugation at 15000 rpm for 5 min, 40 μ l aliquots of this solution were analyzed using LC/MS, as previously reported (Ogawa-Ohnishi *et al.*, 2013). The mass spectra were obtained by scanning the selected ion [(PGVOOS)₃+Ala₁: *m/z* 1849.6] in zoom scan mode.

Double mutant analysis

To select the *plenty har1-7* homozygous double mutant, each plant was checked for the presence of an amplified polymorphic sequence marker in *har1-7* (a G1044A change in the *HAR1* CDS causing a W348 stop codon) (Magori *et al.*, 2009). Deletion of the *plenty* locus was detected using the primers listed in [Supplementary Table S2](#). Nodules and other root phenotypes were counted and measured at 28 DAI.

Gene expression analysis

Total RNA was isolated from each plant tissue at selected time points using an RNeasy Plant Mini Kit (Qiagen), and the first-strand cDNA was prepared using a QuantiTect Reverse Transcription Kit (Qiagen). Reverse transcription-quantitative PCR analysis was performed using an ABI Prism 7000 (Applied Biosystems) with THUNDERBIRD SYBR qPCR Mix (Toyobo) or with a QuantiTect SYBR Green RT-PCR Kit (Qiagen), according to the manufacturers' protocols. *EF-1a* (GNf095a12) expression was used as the reference (Groth *et al.*, 2010). The relative expression levels were calculated using the $\Delta\Delta$ Ct method (Livak and Schmittgen, 2001). The primers used in the expression analysis are shown in [Supplementary Table S2](#). The data are presented as the mean \pm SD of three biological replicates or three technical replicates.

Boxplot analysis

Boxplot analyses were performed in R using ggplot2 or basic R plotting commands. In the boxplots, the upper and lower 'hinges' correspond to the first and third quartiles. The upper whisker extends from the hinge to the highest value within 1.5 \times the interquartile range (IQR) between the first and third quartiles, while the lower whisker extends from the hinge to the lowest value within 1.5 \times IQR. Outliers (data beyond the end of the whiskers) are plotted as points.

Results

Identification of the *PLENTY* gene and phylogenetic analysis

The *plenty* mutant has two characteristic phenotypes, an increased number of nodules and short roots (Yoshida *et al.*, 2010). We previously reported that the *plenty* locus is located between markers TM0002 and TM0324 on the long arm of chromosome II in *L. japonicus*. We narrowed down the region of interest using map-based cloning utilizing a larger mapping population of 1087 F₂ plants ([Supplementary Fig. S1](#)). A genomic PCR analysis of the region between marker TM0308 and the newly developed marker EY005 ([Supplementary Table S1](#))

revealed an ~16 kb deletion spanning two protein-coding genes, CM0308.590.r2.d/Lj2g3v3022950 encoding a putative telomerase-binding protein and CM0308.600.r2.d/Lj2g3v3022970 (<http://www.kazusa.or.jp/lotus/>). The latter gene, which we named *PLENTY*, was orthologous to *MtRDN1* (Supplementary Fig. S2; Schnabel *et al.*, 2011). Similar to *M. truncatula*, two other *PLENTY* paralogs termed *PLENTY2* and *PLENTY3*, were also identified in *L. japonicus*, and the three genes were phylogenetically divided into three related groups (Supplementary Fig. S2). There are no Arabidopsis homologs of *LjPLENTY* and *MtRDN1*; instead, there is a Brassicaceae-specific clade of *PLENTY*-like genes that are closely related to the group containing *LjPLENTY3* and *MtRDN3* (Schnabel *et al.*, 2011; Ogawa-Ohnishi *et al.*, 2013; Xu *et al.*, 2015). To explore further the Brassicaceae-specific evolution of the *PLENTY* genes, we performed a phylogenetic analysis using genes from *Brassica rapa*, *Carica papaya* (papaya), *Gossypium raimondii* (cotton), and *Eucalyptus grandis* (eucalyptus), acquired from the Phytozome database (<http://www.phytozome.net/>), as well as the same data set used in the study of *MtRDN1* (Schnabel *et al.*, 2011). Among these plants, all *PLENTY* homologs from the eudicots, except for those from *B. rapa*, were classified into groups 1–3.

Nodule number and the non-symbiotic short-root phenotype of plenty were complemented by PLENTY expression

The *plenty* mutant has an increased number of nodules and shorter roots in both symbiotic and non-symbiotic conditions (Yoshida *et al.*, 2010). We generated stably transformed *plenty* mutants harboring the *PLENTY* CDS under the control of the *LjUBIQUITIN* promoter or an empty vector (as the control) and observed their phenotypes in both inoculated and non-inoculated conditions. The significantly increased numbers of nodules and short primary roots of *plenty* were rescued by the expression of *PLENTY* CDS in all three independent T₃ transgenic lines, but not by the empty vector control (Fig. 1). The rescued primary root length was also observed in the non-inoculated condition (Fig. 1E, G). There were no significant differences in the number of first-order lateral roots (i.e. lateral roots emerging from the primary root) in the complemented plants (Supplementary Fig. S3). These results indicate that *PLENTY* functions not only in inhibiting nodulation and but also in primary root elongation, in both the presence and absence of rhizobia. As previously reported, *plenty* tends to form increased numbers of larger nodules (Yoshida *et al.*, 2010); therefore, we separately counted small nodules (<0.5 mm in diameter) and large nodules (>0.5 mm in diameter) to evaluate the complementation. The number of large nodules rather than small nodules was significantly reduced in the complemented lines (Fig. 1F).

PLENTY is localized to the Golgi network

To assess the function of *PLENTY*, we next investigated its subcellular localization using a series of constructs expressing *PLENTY*-GFP fusion proteins. Since the N-terminal amino acid sequence of *MtRDN1* was previously predicted to be a signal peptide (SP) for the secretory pathway (Schnabel *et al.*, 2011),

we generated three kinds of constructs fused to GFP: full-length *PLENTY* (Full-*PLENTY*-GFP), *PLENTY* lacking the first 46 amino acids of the N-terminal region including secretory peptides and the transmembrane domain (Δ N1-*PLENTY*-GFP), and only the first 58 amino acids of the N-terminal region of *PLENTY* (N-GFP) (Supplementary Appendix S2). We first examined the localization of GFP and Full-*PLENTY*-GFP constructs following their introduction into onion epidermal cells (Fig. 2B, C) and *L. japonicus* root cells (Supplementary Fig. S4) using particle bombardment. Full-*PLENTY*-GFP was visible in the intracellular punctate structures. We next examined the *Agrobacterium* infiltration of *N. benthamiana* leaves and observed the same punctate localization of Full-*PLENTY*-GFP and N-GFP. To analyze these localization patterns in detail, we compared them with the localization of a mCherry-fused *cis*-Golgi marker, soybean α -1,2-mannosidase I (Nebenführ *et al.*, 1999; Saint-Jore-Dupas *et al.*, 2006; Nelson *et al.*, 2007). The localization of Full-*PLENTY*-GFP and N-GFP overlapped with that of the *cis*-Golgi marker (Fig. 2D–L), as well as the previous localizations reported for its orthologs *AtHPAT1* and *MtRDN1* (Ogawa-Ohnishi *et al.*, 2013; Kassaw *et al.*, 2017). In addition, the Golgi localization of N-GFP, which contrasts with the cytoplasmic or nuclear localization of Δ N1-*PLENTY*-GFP (Supplementary Fig. S4), suggests that the N-terminal (SP) region is necessary and sufficient for targeting *PLENTY* to the Golgi.

In vitro detection of PLENTY enzymatic activities

To determine whether *PLENTY* possess HPAT activity, we examined the enzymatic activity *in vitro* using yeast-expressed recombinant protein. A secretory signal and a transmembrane domain are predicted in the N-terminal region of *PLENTY* (Supplementary Appendix S2). Considering the difficulty in membrane protein purification, we designed not only Full-*PLENTY* but also two N-terminally deleted forms of *PLENTY*, Δ N1-*PLENTY* lacking the first 46 amino acids and Δ N2-*PLENTY* lacking the first 25 amino acids (Supplementary Appendix S2). Western blotting using an antibody to FLAG (anti-FLAG) demonstrated that all three recombinant proteins, Full-*PLENTY* (41.6 kDa), Δ N2-*PLENTY* (38.8 kDa), and Δ N1-*PLENTY* (36.4 kDa), were successfully expressed and collected in the microsomal membrane fractions (Fig. 3A). These fractions were then incubated with a synthetic tandem repeat peptide (PGVOOS)₃, a previously developed substrate for detecting *AtHPAT* activity based on the native PSY1 peptide in Arabidopsis (Amano *et al.*, 2007; Ogawa-Ohnishi *et al.*, 2013), in the presence of UDP- β -L-arabinofuranose (Araf). A subsequent LC/MS analysis revealed that these *PLENTY* proteins catalyzed the arabinosylation of the peptide substrate (Fig. 3B).

Hypernodulation of the plenty mutant was suppressed by the constitutive expression of CLE-RS1 and CLE-RS2 but not CLE-RS3

Although its native substrates have still not been identified, the HPAT activity of *PLENTY* led us to speculate that *PLENTY* modifies the CLE-RS1/2/3 peptides, because of their function in AON (Okamoto *et al.*, 2009; Nishida *et al.*, 2016). Hence, we

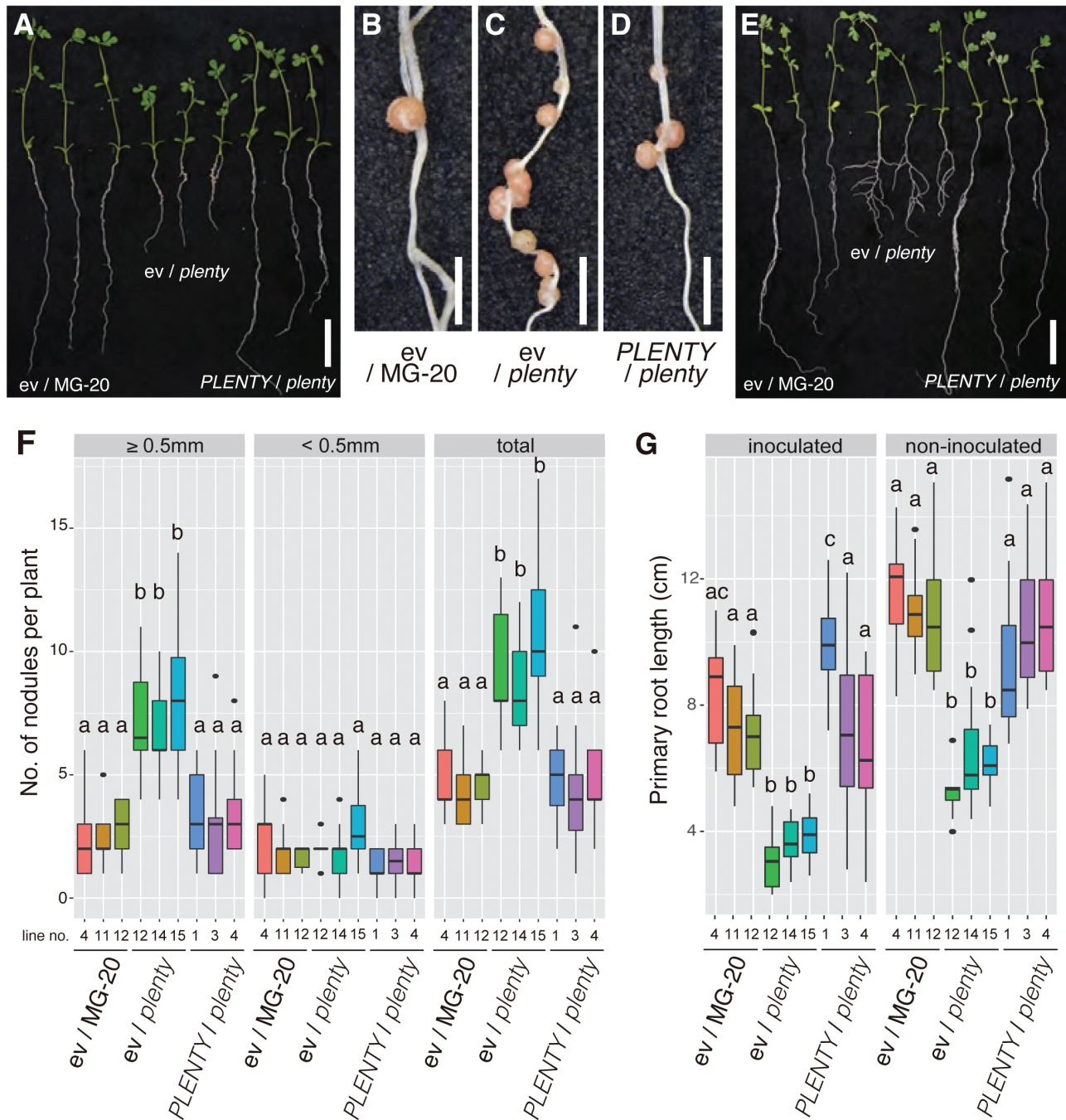


Fig. 1. Complementation of *plenty*. (A) *Rhizobium*-inoculated MG-20 plants stably transformed with the empty vector pUB-GW-GFP (*ev*/MG-20), a *plenty* mutant transformed with the empty vector (*ev*/*plenty*), and a *plenty* mutant transformed with pUB-GW-Full-*PLENTY* (*PLENTY*/*plenty*) at 14 days after inoculation (DAI) with *M. loti* MAFF303099. Magnified images of the nodulated regions of the *ev*/MG-20 (B), *ev*/*plenty* (C), and *PLENTY*/*plenty* (D) plants are shown. (E) Non-inoculated plants of *ev*/MG-20, *ev*/*plenty*, and *PLENTY*/*plenty* at 21 days after germination (DAG). (F) Boxplots of the nodule numbers [≥ 0.5 mm diameter (left), < 0.5 mm diameter (middle), and total (right)] of the individual inoculated T_3 transgenic lines ($n \geq 10$). (G) Boxplots of the primary root length of the inoculated T_3 transgenic plants at 14 DAI (left) and the non-inoculated T_3 transgenic plant at 21 DAG (right). Scale bars=2 cm in (A, E) and 2 mm in (B–D). Different lower case letters represent statistically significant differences ($P < 0.05$; Tukey's HSD). Experiments were performed in triplicate ($n \geq 10$ in each trial).

investigated the nodule suppression effects introduced by the constitutive expression of *CLE-RS1/2/3* in the *plenty* mutant background using hairy root transformation. We hypothesized that if *PLENTY* mediates the arabinosylation of *CLE-RS1/2/3*, and if this modification is critical for their activity, the nodule suppression effect arising from the constitutive expression of *CLE-RS1/2/3* would be abolished in the *plenty* mutant, as

was observed in *har1* (Okamoto *et al.*, 2009) and similarly for *CLE12* expression in *Mtrdn1* (Kassaw *et al.*, 2017). All three $35S::CLE-RS$ ($35S::CLE-RS1/2/3$) constructs suppressed nodulation in the wild type in comparison with the negative controls $35S::GUS$ and $35S::CLE3$. Unexpectedly, however, in *plenty*, the increased nodulation was significantly suppressed by two of the *CLE-RS* constructs, $35S::CLE-RS1$ and $35S::CLE-RS2$

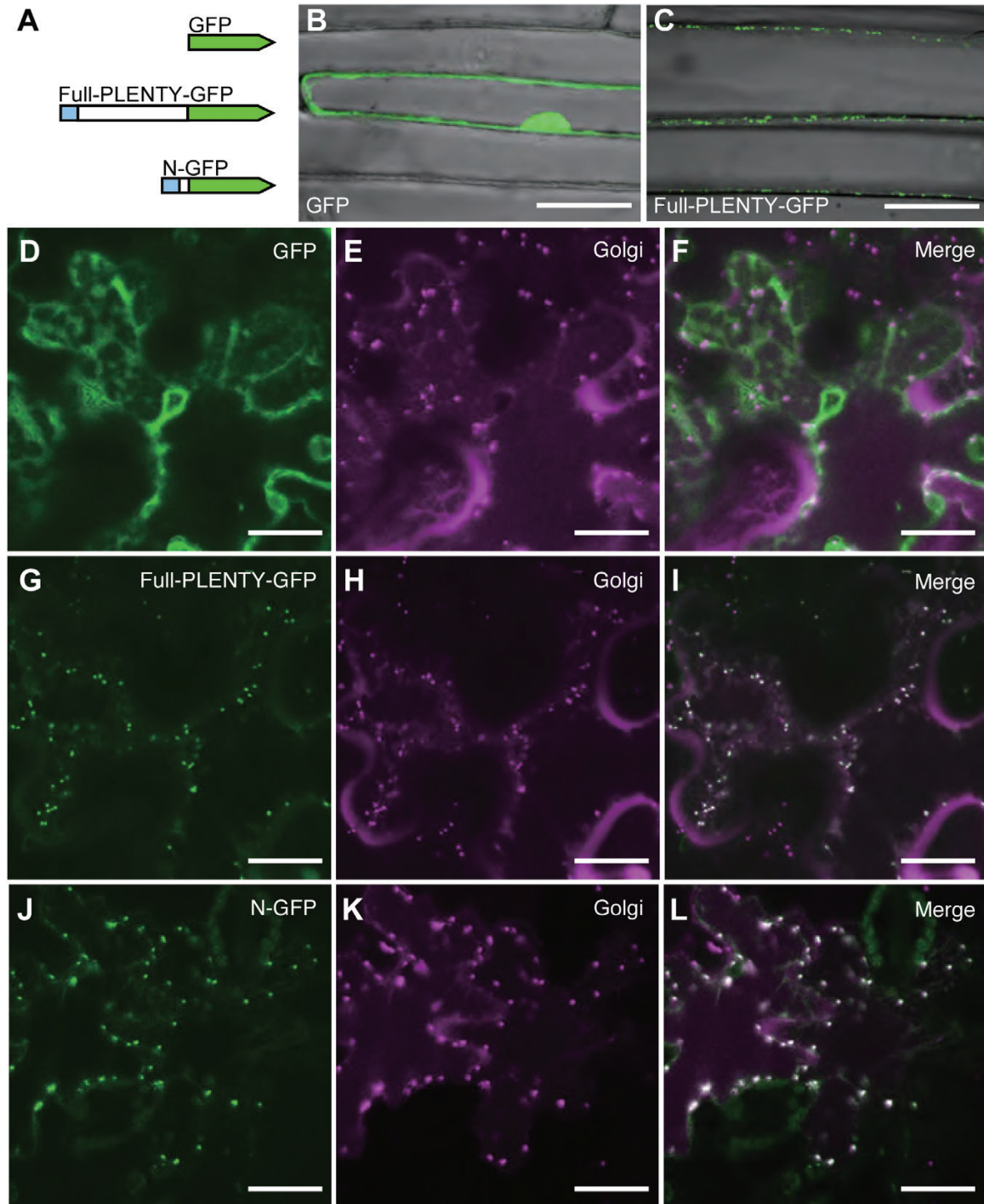


Fig. 2. Subcellular localization of PLENTY-GFP fusion proteins. (A) Overview of the three GFP fusion protein constructs; GFP, Full-PLENTY-GFP, and N-GFP containing the first 58 amino acids of the N-terminal region of PLENTY. PLENTY has a putative secretory signal peptide at the N-terminus (shown in blue). (B–L) Confocal microscopic images of the localization of a series of PLENTY-GFP fusion proteins driven by the CaMV 35S promoter. (B, C) The transient expression in onion epidermal cells transformed using particle bombardment. (D–L) Transient expression in *N. benthamiana* pavement cells co-expressing the mCherry-fused *cis*-Golgi marker, transformed using *A. tumefaciens* infiltration. The constructs used for each analysis are shown in each panel. Merged images show the cytoplasmic localization of GFP (F) and the Golgi localization of Full-PLENTY-GFP and N-GFP (I, L). Scale bars=50 μm in (B, C) and 25 μm in (D–L). Similar GFP localization was observed in >10 transformed cells.

(Fig. 4), although the degree of suppression was stronger in *35S::CLE-RS1* than in *35S::CLE-RS2*. Thus, the constitutive expression of *CLE-RS1/2* maintains sufficient biological activity to repress nodulation, even in *plenty*. On the other hand, the suppression effect of *35S::CLE-RS3* is completely abolished in *plenty*, indicating the involvement of PLENTY in the arabinosylation of *CLE-RS3* rather than that of *CLE-RS1/2*.

Increased nodulation is an additive phenotype in the plenty har1 double mutant, compared with the single mutants

Although it is unclear whether the *CLE-RS1/2* peptides are substrates of PLENTY, the ligand-receptor interaction between *CLE-RS1/2* and HAR1 has been clearly defined previously

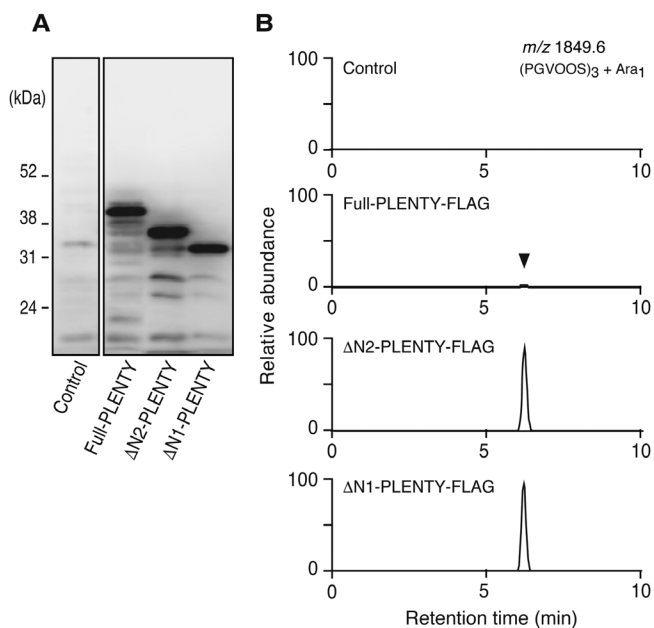


Fig. 3. Identification of the HPAT activity of PLENTY *in vitro*. (A) Western blots of microsomal proteins in yeast expressing C-terminally FLAG-fused PLENTY proteins [Full-PLENTY (41.6 kDa), Δ N2-PLENTY with the first 25 amino acids deleted (38.8 kDa), or Δ N1-PLENTY with the first 46 amino acids deleted (36.4 kDa)], probed using an anti-FLAG antibody. (B) Identification of HPAT activity of the three recombinant PLENTY proteins. The synthetic substrate peptide (PGVOOS)₃ was incubated with the FLAG-tag-fused recombinant proteins in the presence of UDP- β -L-Araf and analyzed using LC/MS. The 1849.6 increase in *m/z* corresponds to the arabinosylation.

(Okamoto *et al.*, 2009, 2013; Sasaki *et al.*, 2014), as the inhibition of nodulation introduced by the constitutive expression of *CLE-RS1/2* occurs in a HAR1-dependent manner. To investigate the genetic interaction between PLENTY and HAR1 further, we generated a *plenty har1-7* double mutant and determined the nodule numbers normalized to the total root length of each plant (Fig. 5). The *har1-7* mutation resulted in the loss of both the transmembrane and kinase domains of HAR1; thus, *har1-7* is a possible null mutant (Magori *et al.*, 2009). The number of large nodules >0.5 mm in diameter and the total number of nodules in *plenty har1-7* were significantly increased relative to those of the *plenty* or *har1-7* single mutants (Fig. 5F). This indicates that PLENTY and HAR1 function in at least partially separate AON pathways. Notably, while the *plenty*, *har1-7*, and *plenty har1-7* mutants all had similar primary root lengths, an additive effect was observed for the shortening of the lateral roots in *plenty har1-7* (Fig. 5G), indicating their involvement in genetically non-overlapping pathways for lateral root elongation. Additionally, the number of first-order lateral roots in the inoculated condition was increased in *har1-7*, as previously reported (Szczygłowski *et al.*, 1998; Wopereis *et al.*, 2000), but decreased in *plenty har1-7*, suggesting that the *plenty* mutation suppressed not only lateral root elongation but also lateral root emergence in *har1-7* (Supplementary Fig. S3).

Discussion

In this study, we cloned *LjPLENTY*, an ortholog of *MtRDN1* and *PsNOD3*, and a homolog of the three *AtHPAT* genes,

and found that, like its orthologs, *LjPLENTY* localizes to the Golgi complex (Ogawa-Ohnishi *et al.*, 2013; Kassaw *et al.*, 2017). Hydroxyproline *O*-arabinosylation is widely observed in secreted Arabidopsis peptides (Shinohara and Matsubayashi, 2010; Matsubayashi, 2014; Kucukoglu and Nilsson, 2015), and studies of HPAT homologs in Arabidopsis, tomato (*Solanum lycopersicum*), and the moss *Physcomitrella patens* have shown that the substrates of these enzymes are involved in diverse aspects of plant development, such as cellular tip growth and meristem maintenance (Ogawa-Ohnishi *et al.*, 2013; Xu *et al.*, 2015; MacAlister *et al.*, 2016). Additionally, the specific gene loss of the group 1 HPATs in the Brassicaceae (Supplementary Fig. S2) (Schmabel *et al.*, 2011) may be associated with the loss of arbuscular mycorrhizal symbiosis in these species (Delaux *et al.*, 2014).

Prior to the discovery of its molecular entity, *PsNOD3* was hypothesized to be involved in generating an unknown root-derived systemic signal that inhibited nodulation based on the findings of a series of grafting experiments (Postma *et al.*, 1988; Caetano-Anollés and Gresshoff, 1990; Li *et al.*, 2009; Novák, 2010). In particular, the hypernodulation on the adventitious roots originating from the wild-type scions on *nod3* rootstocks indicated that the decreased production of the systemic signal affected both wild-type and *nod3* roots. These previous reports also support the subsequent identification of CLE peptides as the root-derived signal. The nodule suppression by the constitutive expression of *MtCLE13* was found to be dependent on *PsNOD3* (Osipova *et al.*, 2012), and a separate study showed that the nodule suppression by *35S::MtCLE12*, but not *35S::MtCLE13*, was dependent on *MtRDN1* (Kassaw *et al.*, 2017). These findings suggest the hypothesis that *LjPLENTY* participates in the maturation of at least one of the *LjCLE-RSs*. In this study, stronger, milder, and no repression of nodulation was found by *35S::CLE-RS1*, *35S::CLE-RS2*, and *35S::CLE-RS3*, respectively, in the *plenty* mutant background. Based on the differential nodule suppression levels, we can only state the order of likelihood that each CLE-RS is the substrate of PLENTY: CLE-RS3 > CLE-RS2 > CLE-RS1 (Supplementary Fig. S5).

The differential requirements for PLENTY between the *CLE-RS* genes are similar to the differential requirements for RDN1 in the functions of *35S::MtCLE12/13* in *Medicago* (Kassaw *et al.*, 2017). The orthologous relationships of the CLEs are not clear because of their short amino acid sequences (Hastwell *et al.*, 2015, 2017), and because the core sequences in the CLE domains of *LjCLE-RS1/2* are shared more with *MtCLE13* than with *MtCLE12* (Imin *et al.*, 2018). This means it is difficult to determine whether the differences in their enzyme-substrate specificities are caused by differences in their amino acid sequences. *MtCLE13* did not suppress nodulation in *nod3* plants, suggesting the requirement for *PsNOD3* (Osipova *et al.*, 2012); but further studies using *PsCLEs* rather than *MtCLE13* are needed for an understanding of the substrate-enzyme specificity in pea. Despite the successful detection of the enzymatic activities of PLENTY using artificially synthesized peptides, it is still unknown whether the arabinosylation of CLE-RS1/2/3 was performed by PLENTY, because the relevant results were based solely on the constitutive expression analysis. So far, the arabinosylation has been detected successfully only in CLE-RS2 (Okamoto *et al.*, 2013); therefore, whether CLE-RS1/3 are arabinosylated has also

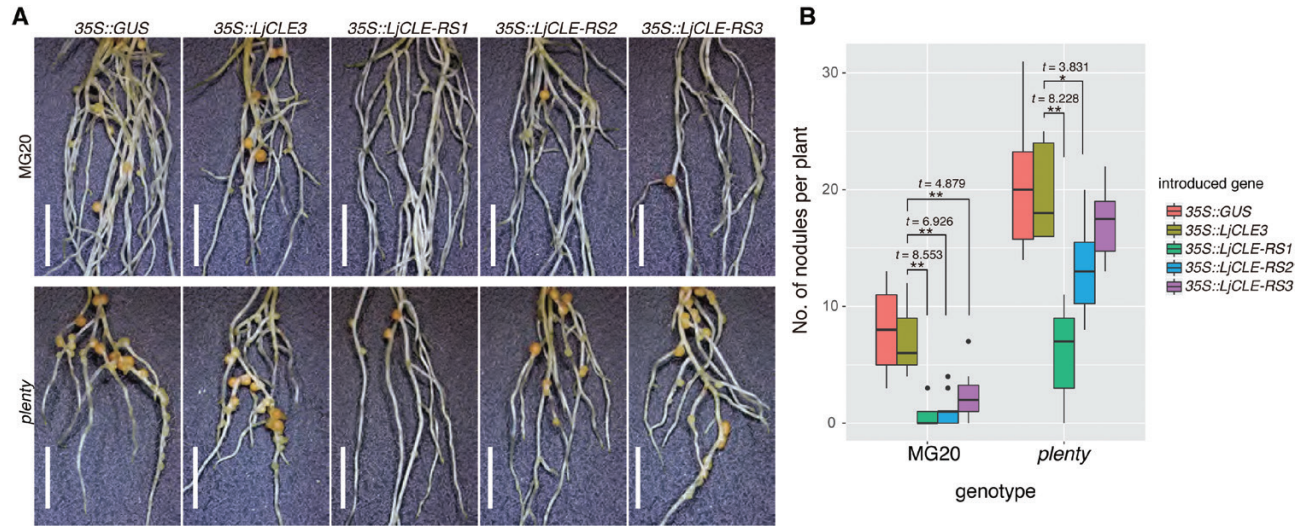


Fig. 4. Hypernodulation of *plenty* was strongly suppressed by *CLE-RS1* and mildly suppressed by *CLE-RS2* but not by *CLE-RS3*. (A) Stereoscopic images of transgenic hairy roots constitutively expressing *GUS* and *LjCLE3* (as a control), *LjCLE-RS1*, *LjCLE-RS2*, or *LjCLE-RS3*. The constructs used for each analysis are shown in each panel. Scale bars=5 mm. (B) Boxplots of the number of nodules per individual transformed plant at 14 DAI with *M. loti* MAFF303099. The genotypes and introduced constructs are indicated on the graph. Statistical analyses were conducted using a two-tailed Welch's *t*-test (** $P < 0.01$, * $P < 0.05$, $n \geq 10$). The black dots represent outliers. Experiments were performed in triplicate ($n \geq 10$ in each trial).

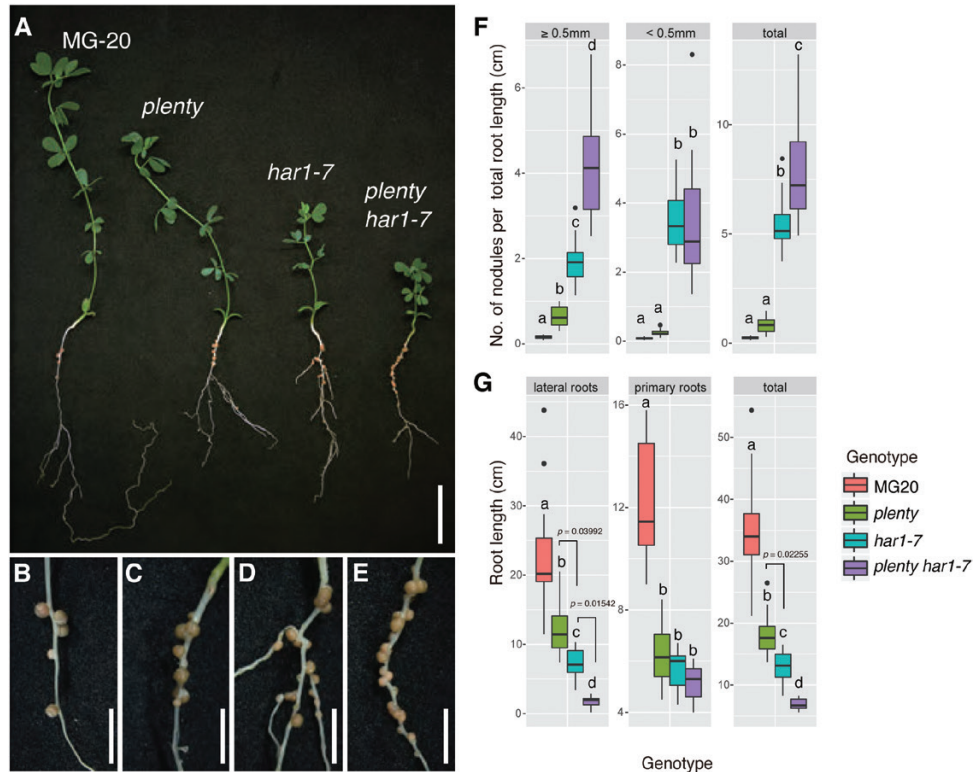


Fig. 5. Additive nodulation of the *plenty har1-7* double mutant. (A) Nodulation in the wild-type (MG-20), *plenty*, *har1-7*, and *plenty har1-7* double mutant plants. (B–E) Magnified images of nodulated roots of the wild type (MG-20) (B), *plenty* (C), *har1-7* (D), and the *plenty har1-7* double mutant (E). (F) Boxplot of the nodule number [≥ 0.5 mm diameter (left), < 0.5 mm diameter (middle), total (right)], normalized by the total root length of each plant, counted at 21 DAI with *M. loti* MAFF303099. (G) Boxplot of the lengths of lateral roots (left), primary roots (middle), and total roots (right) of each plant, measured for normalization in (F). Scale bars=2 cm in (A) and 5 mm in (B–E). The values of the total nodule numbers were used for the statistical analysis in (F). Different lower case letters represent statistically significant differences ($P < 0.05$; Tukey's HSD; $n = 14$). $0.01 < P < 0.05$ are denoted on the graph. The black dots represent outliers. Experiments were performed in triplicate ($n \geq 10$ in each trial).

remained obscure (Supplementary Fig. S5). In conclusion, we cannot completely exclude the possibility that *LjCLE-RS1/2* are the substrates of PLENTY, but the *CLE-RS1/2/3-HAR1* signaling pathway can be divided into PLENTY-dependent

and PLENTY-independent pathways, namely PLENTY-independent for *CLE-RS1*, partially dependent for *CLE-RS2*, and strongly dependent for *CLE-RS3* peptides (Supplementary Fig. S5). To evaluate the contribution of various enzymes to the

modification of the CLE peptides accurately, assays to detect the modification levels of *in vivo* native peptides in respective single, double, and triple mutants of the three PLENTY paralogs should be performed in future studies. Alternatively, a loss-of-function analysis of the *CLE-RS* genes together with the PLENTY paralogs will provide important information.

Based on the additive nodules of the *plenty har1* double mutant, we propose that PLENTY and HAR1 at least partially function in separate AON pathways. First, this additive phenotype would be caused by the milder hypernodulation of *plenty* rather than that of *har1*. This milder phenotype may be affected by the functional redundancy among the three paralogs, as previously suggested for other species (Ogawa-Ohnishi *et al.*, 2013; MacAlister *et al.*, 2016; Kassaw *et al.*, 2017). Thus, the PLENTY-independent nodule suppression by the constitutively expressed *CLE-RS1/2* may be dependent on PLENTY2/3. As we expected, the expression patterns of PLENTY2 and PLENTY3 during nodulation were similar to that of PLENTY (Supplementary Figs S2, S6), as was previously shown for *MtRDN2/3* (Schnabel *et al.*, 2011). Nevertheless, the increased number of nodules in the *plenty har1-7* double mutant raises the possibility that PLENTY provokes AON independently of HAR1. In fact, the *MtSUNN*-independent AON pathway has been discussed before (Kassaw *et al.*, 2015), based on the persistent suppression of excessive nodule formation in *Mtsunn*; however, alternative receptors functioning in a completely HAR1-independent manner have not yet been identified. All known candidate receptors for CLE peptides, *LjKLV*, *LjCLV2/MtCLV2/PsSYM28*, and *LjCRN/MtCRN*, have consistently been thought to interact with *LjHAR1/MtSUNN/PsSYM29* in the same genetic pathway (Miyazawa *et al.*, 2010; Krusell *et al.*, 2011; Crook *et al.*, 2016). We therefore postulate that other unknown LRR-RLKs function in the PLENTY-dependent and HAR1-independent pathway (Supplementary Fig. S5).

Finally, we considered the potential substrates of PLENTY functioning in a HAR1-independent manner. Aside from *CLE-RS1/2/3*, the most plausible candidates are the other CLE peptides, including *LjCLE40* (Nishida *et al.*, 2016; Hastwell *et al.*, 2017), the C-TERMINALLY ENCODED PEPTIDES (CEPs), and other related peptides found to be involved in nodulation in *Medicago* (de Bang *et al.*, 2017; Patel *et al.*, 2017); in particular, *MtCEP1* functioning in promoting nodulation under nitrogen-limited conditions (Imin *et al.*, 2013; Mohd-Radzman *et al.*, 2016). Moreover, the tri-arabinosylation of the *MtCEP1* proline reduced or eliminated the nodule-promoting effect of this peptide (Patel *et al.*, 2017), which contrasts with the necessity of arabinosylation for *LjCLE-RS2* or *MtCLE12/13* activities (Okamoto *et al.*, 2013; Imin *et al.*, 2018). *MtRDN1* may therefore keep *MtCEP1* inactive to inhibit increased nodulation; thus, the *MtCEP1* ortholog may actually be a substrate of PLENTY. Additionally, the inhibition of lateral root emergence by *MtCEP1* was abolished by non-arabinosylated *MtCEP1* (Patel *et al.*, 2017). The reduced number of emerged lateral roots of the *plenty har1-7* may be caused by accumulation of the non-arabinosylated *CEP1*-like peptide (Supplementary Fig. S3). Also, other unidentified substrates of PLENTY may have effects on the shorter primary root of *plenty* (Fig. 1) or the shorter and reduced lateral

root of *plenty har1-7* (Fig. 5; Supplementary Fig. S3). The arabinosylated peptides involved in root architecture are strong candidates to be these substrates (Corcilius *et al.*, 2017; Patel *et al.*, 2017; Oh *et al.*, 2018). Interestingly, the *MtCEP1* receptor, compact root architecture 2, acts on the shoot for nodulation but on the root for lateral root development through different pathways (Huault *et al.*, 2014; Mohd-Radzman *et al.*, 2016). *LjHAR1* is also a common factor involved in both nodulation control and non-symbiotic root development (Wopereis *et al.*, 2000), but its ligand and shoot/root dependency responding to symbiotic and non-symbiotic phenotype were unknown. Identifying substrates of PLENTY will lead to a further understanding of how nodulation and root architecture are controlled at the same time via HAR1 or other receptors.

Supplementary data

Supplementary data are available at JXB online.

Fig. S1. Identification of the *plenty* locus.

Fig. S2. Phylogenetic tree of the PLENTY family in land plants.

Fig. S3. First-order lateral roots in the complementation test and the *plenty har1-7* double mutant analysis.

Fig. S4. The N-terminal region of PLENTY is necessary and sufficient for localization to the Golgi.

Fig. S5. A working model of PLENTY in the negative control of nodulation.

Fig. S6. The gene expression patterns of the PLENTY paralogs.

Table S1. Newly developed genetic markers for the map-based cloning of PLENTY.

Table S2. Primers used in this study.

Appendix S1. FASTA file of amino acid sequences used for the phylogenetic analysis.

Appendix S2. The deletion series of PLENTY proteins used in this study.

Acknowledgements

We thank Shoji Mano, Michitaro Shibata, and the Spectrography and Bioimaging Facility of NIBB Core Research Facilities for their technical support; Norio Suganuma, Saori Tomisawa, Takema Sasaki, Shoji Mano, Tsuyoshi Nakagawa, Kenji Yamada, Shino Goto-Yamada, Kentaro Tamura, Mikio Nishimura, and Ikuko Hara-Nishimura for providing plant seeds or vectors; and Shoji Mano and Masanao Sato for their valuable comments. This work was supported by the Japan Society for the Promotion of Science (JSPS) Grant-in-Aid for JSPS Fellow [grant nos 25-3940 to EY and 17J02948 to HN], and the Ministry of Education, Culture, Sports, Science and Technology Grants-in-Aid for Scientific Research [grant nos 25114519, 16H01457, and 18H04773 to TS, 25221105, 18H05274, and 15H05957 to YM and 22128006 to MK]. The authors have no conflicts of interest to declare.

References

- Amano Y, Tsubouchi H, Shinohara H, Ogawa M, Matsubayashi Y. 2007. Tyrosine-sulfated glycopeptide involved in cellular proliferation and expansion in *Arabidopsis*. *Proceedings of the National Academy of Sciences, USA* **104**, 18333–18338.
- Broughton WJ, Dilworth MJ. 1971. Control of leghaemoglobin synthesis in snake beans. *Biochemical Journal* **125**, 1075–1080.

- Caetano-Anollés G, Gresshoff PM.** 1990. Early induction of feedback regulatory responses governing nodulation in soybean. *Plant Science* **71**, 69–81.
- Caetano-Anollés G, Gresshoff PM.** 1991. Efficiency of nodule initiation and autoregulatory responses in a supernodulating soybean mutant. *Applied and Environmental Microbiology* **57**, 2205–2210.
- Corcilus L, Hastwell AH, Zhang M, Williams J, Mackay JP, Gresshoff PM, Ferguson BJ, Payne RJ.** 2017. Arabinosylation modulates the growth-regulating activity of the peptide hormone CLE40a from soybean. *Cell Chemical Biology* **24**, 1347–1355.
- Crook AD, Schnabel EL, Frugoli JA.** 2016. The systemic nodule number regulation kinase SUNN in *Medicago truncatula* interacts with MtCLV2 and MtCRN. *The Plant Journal* **88**, 108–119.
- de Bang TC, Lundquist PK, Dai X, et al.** 2017. Genome-wide identification of medicago peptides involved in macronutrient responses and nodulation. *Plant Physiology* **175**, 1669–1689.
- Delaux PM, Varala K, Edger PP, Coruzzi GM, Pires JC, Ané JM.** 2014. Comparative phylogenomics uncovers the impact of symbiotic associations on host genome evolution. *PLoS Genetics* **10**, e1004487.
- Delves AC, Mathews A, Day DA, Carter AS, Carroll BJ, Gresshoff PM.** 1986. Regulation of the soybean–*Rhizobium* nodule symbiosis by shoot and root factors. *Plant Physiology* **82**, 588–590.
- Djordjevic MA, Oakes M, Wong CE, Singh M, Bhalla P, Kusumawati L, Imin N.** 2011. Border sequences of *Medicago truncatula* CLE36 are specifically cleaved by endoproteases common to the extracellular fluids of *Medicago* and soybean. *Journal of Experimental Botany* **62**, 4649–4659.
- Edgar RC.** 2004. MUSCLE: multiple sequence alignment with high accuracy and high throughput. *Nucleic Acids Research* **32**, 1792–1797.
- Groth M, Takeda N, Perry J, et al.** 2010. NENA, a *Lotus japonicus* homolog of Sec13, is required for rhizodermal infection by arbuscular mycorrhiza fungi and rhizobia but dispensable for cortical endosymbiotic development. *The Plant Cell* **22**, 2509–2526.
- Hastwell AH, de Bang TC, Gresshoff PM, Ferguson BJ.** 2017. Author Correction: CLE peptide-encoding gene families in *Medicago truncatula* and *Lotus japonicus*, compared with those of soybean, common bean and *Arabidopsis*. *Scientific Reports* **7**, 15474.
- Hastwell AH, Gresshoff PM, Ferguson BJ.** 2015. The structure and activity of nodulation-suppressing CLE peptide hormones of legumes. *Functional Plant Biology* **42**, 229–238.
- Huault E, Laffont C, Wen J, Mysore KS, Ratet P, Duc G, Frugier F.** 2014. Local and systemic regulation of plant root system architecture and symbiotic nodulation by a receptor-like kinase. *PLoS Genetics* **10**, e1004891.
- Imin N, Mohd-Radzman NA, Ogilvie HA, Djordjevic MA.** 2013. The peptide-encoding CEP1 gene modulates lateral root and nodule numbers in *Medicago truncatula*. *Journal of Experimental Botany* **64**, 5395–5409.
- Imin N, Patel N, Corcilus L, Payne RJ, Djordjevic MA.** 2018. CLE peptide tri-arabinosylation and peptide domain sequence composition are essential for SUNN-dependent autoregulation of nodulation in *Medicago truncatula*. *New Phytologist* **218**, 73–80.
- Kassaw T, Bridges W Jr, Frugoli J.** 2015. Multiple autoregulation of nodulation (AON) signals identified through split root analysis of *Medicago truncatula sunn* and *rdn1* mutants. *Plants* **4**, 209–224.
- Kassaw T, Nowak S, Schnabel E, Frugoli J.** 2017. ROOT DETERMINED NODULATION1 is required for *M. truncatula* CLE12, but not CLE13, peptide signaling through the SUNN receptor kinase. *Plant Physiology* **174**, 2445–2456.
- Kinkema M, Gresshoff PM.** 2008. Investigation of downstream signals of the soybean autoregulation of nodulation receptor kinase GmNARK. *Molecular Plant-Microbe Interactions* **21**, 1337–1348.
- Kinoshita A, Betsuyaku S, Osakabe Y, Mizuno S, Nagawa S, Stahl Y, Simon R, Yamaguchi-Shinozaki K, Fukuda H, Sawa S.** 2010. RPK2 is an essential receptor-like kinase that transmits the CLV3 signal in *Arabidopsis*. *Development* **137**, 3911–3920.
- Kosslak RM, Bohlool BB.** 1984. Suppression of nodule development of one side of a split-root system of soybeans caused by prior inoculation of the other side. *Plant Physiology* **75**, 125–130.
- Krusell L, Madsen LH, Sato S, et al.** 2002. Shoot control of root development and nodulation is mediated by a receptor-like kinase. *Nature* **420**, 422–426.
- Krusell L, Sato N, Fukuhara I, et al.** 2011. The *Clavata2* genes of pea and *Lotus japonicus* affect autoregulation of nodulation. *The Plant Journal* **65**, 861–871.
- Kucukoglu M, Nilsson O.** 2015. CLE peptide signaling in plants—the power of moving around. *Physiologia Plantarum* **155**, 74–87.
- Le SQ, Gascuel O.** 2008. An improved general amino acid replacement matrix. *Molecular Biology and Evolution* **25**, 1307–1320.
- Li D, Kinkema M, Gresshoff PM.** 2009. Autoregulation of nodulation (AON) in *Pisum sativum* (pea) involves signalling events associated with both nodule primordia development and nitrogen fixation. *Journal of Plant Physiology* **166**, 955–967.
- Lin YH, Ferguson BJ, Kereszt A, Gresshoff PM.** 2010. Suppression of hypernodulation in soybean by a leaf-extracted, NARK- and Nod factor-dependent, low molecular mass fraction. *New Phytologist* **185**, 1074–1086.
- Livak KJ, Schmittgen TD.** 2001. Analysis of relative gene expression data using real-time quantitative PCR and the 2(-Delta Delta C(T)) Method. *Methods* **25**, 402–408.
- MacAlister CA, Ortiz-Ramírez C, Becker JD, Feijó JA, Lippman ZB.** 2016. Hydroxyproline O-arabinosyltransferase mutants oppositely alter tip growth in *Arabidopsis thaliana* and *Physcomitrella patens*. *The Plant Journal* **85**, 193–208.
- Maekawa T, Kusakabe M, Shimoda Y, Sato S, Tabata S, Murooka Y, Hayashi M.** 2008. Polyubiquitin promoter-based binary vectors for overexpression and gene silencing in *Lotus japonicus*. *Molecular Plant-Microbe Interactions* **21**, 375–382.
- Magori S, Kawaguchi M.** 2009. Long-distance control of nodulation: molecules and models. *Molecules and Cells* **27**, 129–134.
- Magori S, Oka-Kira E, Shibata S, Umehara Y, Kouchi H, Hase Y, Tanaka A, Sato S, Tabata S, Kawaguchi M.** 2009. Too much love, a root regulator associated with the long-distance control of nodulation in *Lotus japonicus*. *Molecular Plant-Microbe Interactions* **22**, 259–268.
- Mano S, Nakamori C, Nito K, Kondo M, Nishimura M.** 2006. The *Arabidopsis* pex12 and pex13 mutants are defective in both PTS1- and PTS2-dependent protein transport to peroxisomes. *The Plant Journal* **47**, 604–618.
- Matsubayashi Y.** 2014. Posttranslationally modified small-peptide signals in plants. *Annual Review of Plant Biology* **65**, 385–413.
- Miyazawa H, Oka-Kira E, Sato N, et al.** 2010. The receptor-like kinase KLAVER mediates systemic regulation of nodulation and non-symbiotic shoot development in *Lotus japonicus*. *Development* **137**, 4317–4325.
- Mohd-Radzman NA, Laffont C, Ivanovici A, Patel N, Reid D, Stougaard J, Frugier F, Imin N, Djordjevic MA.** 2016. Different pathways act downstream of the CEP peptide receptor CRA2 to regulate lateral root and nodule development. *Plant Physiology* **171**, 2536–2548.
- Mortier V, Den Herder G, Whitford R, Van de Velde W, Rombauts S, D'Haeseleer K, Holsters M, Goormachtig S.** 2010. CLE peptides control *Medicago truncatula* nodulation locally and systemically. *Plant Physiology* **153**, 222–237.
- Mortier V, Fenta BA, Martens C, Rombauts S, Holsters M, Kunert K, Goormachtig S.** 2011. Search for nodulation-related CLE genes in the genome of *Glycine max*. *Journal of Experimental Botany* **62**, 2571–2583.
- Nakagawa T, Kurose T, Hino T, Tanaka K, Kawamukai M, Niwa Y, Toyooka K, Matsuoka K, Jinbo T, Kimura T.** 2007. Development of series of gateway binary vectors, pGWBs, for realizing efficient construction of fusion genes for plant transformation. *Journal of Bioscience and Bioengineering* **104**, 34–41.
- Nebenführ A, Gallagher LA, Dunahay TG, Frohlick JA, Mazurkiewicz AM, Meehl JB, Staehelin LA.** 1999. Stop-and-go movements of plant Golgi stacks are mediated by the acto-myosin system. *Plant Physiology* **121**, 1127–1142.
- Nelson BK, Cai X, Nebenführ A.** 2007. A multicolored set of in vivo organelle markers for co-localization studies in *Arabidopsis* and other plants. *The Plant Journal* **51**, 1126–1136.
- Nishida H, Handa Y, Tanaka S, Suzaki T, Kawaguchi M.** 2016. Expression of the CLE-RS3 gene suppresses root nodulation in *Lotus japonicus*. *Journal of Plant Research* **129**, 909–919.
- Nishida H, Suzaki T.** 2018. Nitrate-mediated control of root nodule symbiosis. *Current Opinion in Plant Biology* **44**, 129–136.
- Nishida H, Tanaka S, Handa Y, et al.** 2018. A NIN-LIKE PROTEIN mediates nitrate-induced control of root nodule symbiosis in *Lotus japonicus*. *Nature Communications* **9**, 499.

- Nishimura R, Hayashi M, Wu GJ, et al.** 2002. HAR1 mediates systemic regulation of symbiotic organ development. *Nature* **420**, 426–429.
- Novák K.** 2010. Early action of pea symbiotic gene NOD3 is confirmed by adventitious root phenotype. *Plant Science* **179**, 472–478.
- Ogawa-Ohnishi M, Matsushita W, Matsubayashi Y.** 2013. Identification of three hydroxyproline O-arabinosyltransferases in *Arabidopsis thaliana*. *Nature Chemical Biology* **9**, 726–730.
- Oh E, Seo PJ, Kim J.** 2018. Signaling peptides and receptors coordinating plant root development. *Trends in Plant Science* **23**, 337–351.
- Okamoto S, Ohnishi E, Sato S, Takahashi H, Nakazono M, Tabata S, Kawaguchi M.** 2009. Nod factor/nitrate-induced CLE genes that drive HAR1-mediated systemic regulation of nodulation. *Plant & Cell Physiology* **50**, 67–77.
- Okamoto S, Shinohara H, Mori T, Matsubayashi Y, Kawaguchi M.** 2013. Root-derived CLE glycopeptides control nodulation by direct binding to HAR1 receptor kinase. *Nature Communications* **4**, 2191.
- Okamoto S, Suzuki T, Kawaguchi M, Higashiyama T, Matsubayashi Y.** 2015. A comprehensive strategy for identifying long-distance mobile peptides in xylem sap. *The Plant Journal* **84**, 611–620.
- Osipova MA, Mortier V, Demchenko KN, Tsyganov VE, Tikhonovich IA, Lutova LA, Dolgikh EA, Goormachtig S.** 2012. Wuschel-related homeobox5 gene expression and interaction of CLE peptides with components of the systemic control add two pieces to the puzzle of autoregulation of nodulation. *Plant Physiology* **158**, 1329–1341.
- Patel N, Mohd-radzman NA, Corcilus L, Crossett B, Connolly A, Payne RJ, Djordjevic MA.** 2017. Diverse peptide hormones affecting root growth identified in the *Medicago truncatula* secreted peptidome. *Molecular & Cellular Proteomics* **61**, 1–50.
- Postma JG, Jacobsen E, Feenstra WJ.** 1988. 3 pea mutants with an altered nodulation studied by genetic-analysis and grafting. *Journal of Plant Physiology* **132**, 424–430.
- Reid DE, Ferguson BJ, Gresshoff PM.** 2011a. Inoculation- and nitrate-induced CLE peptides of soybean control NARK-dependent nodule formation. *Molecular Plant-Microbe Interactions* **24**, 606–618.
- Reid DE, Ferguson BJ, Hayashi S, Lin YH, Gresshoff PM.** 2011b. Molecular mechanisms controlling legume autoregulation of nodulation. *Annals of Botany* **108**, 789–795.
- Reid DE, Hayashi S, Lorenc M, Stiller J, Edwards D, Gresshoff PM, Ferguson BJ.** 2012. Identification of systemic responses in soybean nodulation by xylem sap feeding and complete transcriptome sequencing reveal a novel component of the autoregulation pathway. *Plant Biotechnology Journal* **10**, 680–689.
- Sagan M, Duc G.** 1996. Sym28 and Sym29, two new genes involved in regulation of nodulation in pea (*Pisum sativum* L.). *Symbiosis* **20**, 229–245.
- Saint-Jore-Dupas C, Nebenführ A, Boulaflois A, Follet-Gueye ML, Plasson C, Hawes C, Driouich A, Faye L, Gomord V.** 2006. Plant N-glycan processing enzymes employ different targeting mechanisms for their spatial arrangement along the secretory pathway. *The Plant Cell* **18**, 3182–3200.
- Sasaki T, Suzaki T, Soyano T, Kojima M, Sakakibara H, Kawaguchi M.** 2014. Shoot-derived cytokinins systemically regulate root nodulation. *Nature Communications* **5**, 4983.
- Schnabel E, Journet EP, de Carvalho-Niebel F, Duc G, Frugoli J.** 2005. The *Medicago truncatula* SUNN gene encodes a CLV1-like leucine-rich repeat receptor kinase that regulates nodule number and root length. *Plant Molecular Biology* **58**, 809–822.
- Schnabel EL, Kassaw TK, Smith LS, Marsh JF, Oldroyd GE, Long SR, Frugoli JA.** 2011. The ROOT DETERMINED NODULATION1 gene regulates nodule number in roots of *Medicago truncatula* and defines a highly conserved, uncharacterized plant gene family. *Plant Physiology* **157**, 328–340.
- Searle IR, Men AE, Laniya TS, Buzas DM, Iturbe-Ormaetxe I, Carroll BJ, Gresshoff PM.** 2003. Long-distance signaling in nodulation directed by a CLAVATA1-like receptor kinase. *Science* **299**, 109–112.
- Shinohara H, Matsubayashi Y.** 2010. Arabinosylated glycopeptide hormones: new insights into CLAVATA3 structure. *Current Opinion in Plant Biology* **13**, 515–519.
- Showalter AM, Basu D.** 2016. Extensin and arabinogalactan-protein biosynthesis: glycosyltransferases, research challenges, and biosensors. *Frontiers in Plant Science* **7**, 814.
- Soyano T, Hirakawa H, Sato S, Hayashi M, Kawaguchi M.** 2014. NODULE INCEPTION creates a long-distance negative feedback loop involved in homeostatic regulation of nodule organ production. *Proceedings of the National Academy of Sciences, USA* **111**, 14607–14612.
- Suzaki T, Yano K, Ito M, Umehara Y, Suganuma N, Kawaguchi M.** 2012. Positive and negative regulation of cortical cell division during root nodule development in *Lotus japonicus* is accompanied by auxin response. *Development* **139**, 3997–4006.
- Suzaki T, Yoro E, Kawaguchi M.** 2015. Leguminous plants: inventors of root nodules to accommodate symbiotic bacteria. *International Review of Cell and Molecular Biology* **316**, 111–158.
- Szczyglowski K, Shaw RS, Wopereis J, Copeland S, Hamburger D, Kasiborski B, Dazzo FB, de Bruijn FJ.** 1998. Nodule organogenesis and symbiotic mutants of the model legume *Lotus japonicus*. *Molecular Plant-Microbe Interactions* **11**, 684–697.
- Takahara M, Magori S, Soyano T, et al.** 2013. Too much love, a novel Kelch repeat-containing F-box protein, functions in the long-distance regulation of the legume–*Rhizobium* symbiosis. *Plant & Cell Physiology* **54**, 433–447.
- Tamura K, Stecher G, Peterson D, Filipski A, Kumar S.** 2013. MEGA6: molecular evolutionary genetics analysis version 6.0. *Molecular Biology and Evolution* **30**, 2725–2729.
- Udvardi M, Poole PS.** 2013. Transport and metabolism in legume–rhizobia symbioses. *Annual Review of Plant Biology* **64**, 781–805.
- Voinnet O, Rivas S, Mestre P, Baulcombe D.** 2003. An enhanced transient expression system in plants based on suppression of gene silencing by the p19 protein of tomato bushy stunt virus. *The Plant Journal* **33**, 949–956.
- Wopereis J, Pajuelo E, Dazzo FB, Jiang Q, Gresshoff PM, De Bruijn FJ, Stougaard J, Szczyglowski K.** 2000. Short root mutant of *Lotus japonicus* with a dramatically altered symbiotic phenotype. *The Plant Journal* **23**, 97–114.
- Xu C, Liberatore KL, MacAlister CA, et al.** 2015. A cascade of arabinosyltransferases controls shoot meristem size in tomato. *Nature Genetics* **47**, 784–792.
- Yoshida C, Funayama-Noguchi S, Kawaguchi M.** 2010. plenty, a novel hypernodulation mutant in *Lotus japonicus*. *Plant & Cell Physiology* **51**, 1425–1435.